International Journal of Research in Science & Technology
Volume 2 | Issue 4 | April 2015 | ISSN: 2349-0845

Reduction of Frequency Offset Using Joint Clock for OFDM Based Cellular Systems over Generalized Fading Channels

S.L.S.Durga[1] , M.V.V.N.Revathi[2], M.J.P.Nayana[3], Md.Aaqila Fathima[4] and K.Murali[5]

[1, 2, 3, 4] B.Tech Students, Department of ECE, Vijaya Institute of Technology for Women, Vijayawada, India.
lakshmichowdary72@gmail.com , nagarevathi94.muddineni@gmail.com , medasanijyothi@gmail.com , aaqilafathima111@gmail.com

[5] Assistant Professor, Department of ECE, Vijaya Institute of Technology for Women, Vijayawada, India.
kalipindimurali@gmail.com

Article Info

Article history:

Received on 1st April 2015
Accepted on 5th April 2015.
Published on 8th April 2015

Keyword:

Carrier Frequency offset, OFDM,
Sampling Clock offset, Synchronization

ABSTRACT

This project addresses the problem of clock synchronization between a base station (BS) and a mobile station (MS). A conventional technique for clock synchronization is that the MS clock is derived from the downlink signal originated from a base station. In cellular systems, a base station and mobile stations need to be synchronized before data exchange. Since the base station clock reference is more accurate, a mobile station typically derives its clock reference from the base station. But the carrier frequency offset due to Doppler shift may have harmful effects on the local clock derivation. This project proposes a joint clock and frequency synchronization technique between a base station and a mobile station, which is effective even with Doppler shift. We derive the joint estimation algorithm by analyzing the phase and the amplitude distortion caused by the sampling frequency offset and the carrier frequency offset. Simulation results showing the effectiveness of the proposed algorithm will also be presented.

Corresponding Author:

K. Murali
Assistant Professor, Department of ECE,
Vijaya Institute of Technology for Women,
Vijayawada, India.
Email Id: kalipindimurali@gmail.com

I. INTRODUCTION

Orthogonal frequency division multiplexing (OFDM) is a transmission method that can achieve high data rates by multicarrier modulation. The wireless local area network standard, IEEE 802.11a, issued by the Institute of Electrical and Electronics Engineers (IEEE), is based on OFDM [1, 2]. Furthermore, OFDM exhibits much better bandwidth efficiency than classical frequency division multiplexing (FDM) provided that the orthogonality of the carriers is preserved[3]. One of the biggest problems with OFDM systems is their sensitivity to frequency offset between oscillators at the transmitter and the receiver which causes ICI due to loss of orthogonality.

A very important aspect in OFDM is time and frequency synchronization. In particular, frequency synchronization is the basis of the orthogonality between frequencies. Loss in frequency synchronization is caused by a number of issues[3]. It can be caused by Doppler shift due to relative motion between the transmitter and the receiver. This is particularly severe when each OFDM frame has a large number of frequencies closely spaced next to each other.

In systems based on the IEEE 802.11a standard, the Doppler effects are negligible when compared to the frequency spacing of more than 300 kHz. What is more important in this situation is the frequency error caused by imperfections in oscillators at the modulator and the demodulator c[4]. These frequency errors cause a frequency offset comparable to the frequency spacing, thus lowering the overall SNR.

So the effects of frequency offset on OFDM systems and frequency offset estimation techniques are needed to be obtained to correct for their effects.

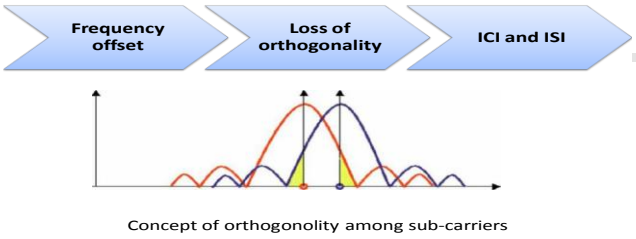

Figure 1. Concept of orthogonality among sub carries

OFDM is a block transmission technique. In the baseband, complex-valued data symbols modulate a large number of tightly grouped carrier waveforms. The transmitted OFDM signal multiplexes several low-rate data streams - each data stream is associated with a given subcarrier[5] The main advantage of this concept in a radio environment is that each of the data streams experiences an almost at fading channel. The *inter symbol interference* (ISI) and *inter carrier interference* (ICI) within an OFDM symbol can be avoided completely with a small loss of transmission energy using the concept of a cyclic prefix.

II. PROPOSED WORK

A. *Offset Estimation Algorithm*

Three types of algorithms are used for offset estimation

1) Algorithms that use pilot tones for estimation (data-aided).

The data-aided category uses a training sequence or pilot symbols for estimation. It has high accuracy and low calculation, but loses the bandwidth and reduces the data transmission speed [6].

2) Algorithms that process the data at the receiver (blind).

These techniques do not waste bandwidth to transmit pilot tones. However, they use less information at the expense of added complexity and degraded performance[7].

3) Algorithms that use the cyclic prefix for estimation

The non-data aided category often uses the cyclic prefix correlation. It doesn't waste bandwidth and reduce the transmission speed, but its estimation range is too small, not suitable for acquisition[8].

B. *Considered Scenario*

i. *CP Based:*

With perfect symbol synchronization, a CFO of ξ results in a phase rotation of $2\pi n\xi/N$ in the received signal[6]. Under the assumption of negligible channel effect, the phase difference between CP and the corresponding rear part of an OFDM symbol (spaced N samples apart) is $2\pi N\xi/N = 2\pi\xi$. Then, the CFO can be found from the phase angle of the product of CP and the corresponding rear part of an OFDM symbol.

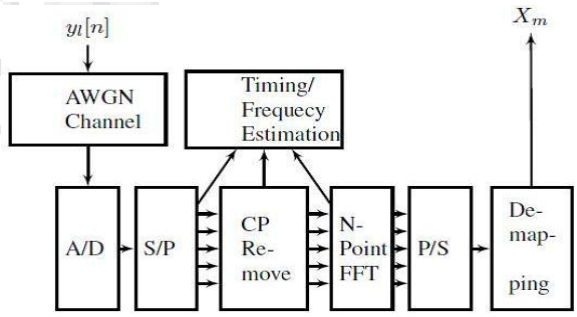

Figure 2: OFDM Receiver block.

ii. *Synchronization Requirements:*

Accurate demodulation and detection of an OFDM signal requires subcarrier orthogonality. Variations of the carrier oscillator, the sample clock or the symbol clock affect the orthogonality of the system, see [7,12]. Whereas sample clock variations below 50 ppm have little effect on the system performance [12], symbol time and frequency offsets may cause inter symbol interference (ISI) and inter carrier interference (ICI) [7, 12] and must usually be

counteracted. Therefore, we assume that the sample clocks of the users and the base station are identical (no offset effects) and we focus on a frequency offset and a symbol time offset. We separately consider their effects on the system performance. In this chapter, the degradation due to frequency offset and some of the techniques to obtain frequency synchronization are discussed. In particular the effect of an error in frequency synchronization on the demodulated signal is considered, and an expression for degradation in terms of Signal-to-Noise Ratio (SNR) is described.

C. *Effects of Frequency offset on OFDM Signals*

Frequency offset comes from a number of sources such as Doppler shift or frequency drifts in the modulator and the demodulator oscillators. The first source of error arises when there is relative motion between transmitter and receiver. In this case, the frequency shift is given by

$$\Delta f = \frac{v}{c} \times f_c \qquad (1)$$

Where v is the relative velocity, c is the speed of light, and f_c is the carrier frequency. Compared to the frequency spacing this shift is negligible. For example, with a carrier frequency of (f_c): 5 GHZ and a velocity of 100 km/h. the offset value is Δf is 1.6 kHz, which is relatively insignificant compared to the carrier spacing of312.5 kHz. The other source of frequency offset is due to frequency errors in the oscillators. The IEEE 802.l1 standard requires the oscillators to have frequency errors within 20 ppm(or $20*10^{-4}$). For a carrier of 5 GHZ, this means a maximum frequency error of

$$|\Delta f_{MAX}| = 2 \times 20 \times 10^{-6} \times 5 \times 10^{9} = 200 \text{ kHz} \qquad (2)$$

Where the factor "2" accounts for the transmitter and receiver having errors with opposite signs. This error is relatively large compared to the frequency spacing of the carrier.

The general approaches to the problem of synchronization consist of a number of steps, including frame detection, carrier frequency offset and sampling error correction. Frame detection is used to determine the symbol boundary needed for correct demodulation. Within each frame, the carrier frequency offset between the transmitter and the receiver causes an unknown phase shift factor[12].

D. *Frequency offset and Inter Carrier Interface (ICE)*

According to the degradation of the SNR, D_{freq}, caused by the frequency offset is approximated

$$D_{freq} \cong \frac{10}{3 \ln 10} (\pi \Delta_f T)^2 \frac{E_b}{N_o} \qquad (3)$$

Where Δ_f is the frequency offset, T is the symbol duration in seconds, E_b is the energy-per bit of the OFDM signal and N_o is the one-sided noise power spectrum density (PSD). The frequency offset has an effect like noise and it degrades the signal-to-noise ratio (SNR), where SNR is the $\frac{E_b}{N_o}$ ratio. Figure below shows the calculated degradation of the SNR due to the frequency offset. For smaller SNR values, the degradation is less than for bigger SNR values

3.ML estimation

Assume that we observe $2N+L$ consecutive samples of $r(k)$, *cf.* Figure3, and that these samples contain one complete ($N + L$) -sample OFDM symbol. The position of this symbol within the observed block of samples, however, is unknown because the channel delay μ is unknown to the receiver. Define the index sets

$$I \triangleq \{\theta, \ldots, \theta + L - 1\}$$
$$I' \triangleq \{\theta + N, \ldots, \theta + N + L - 1\},$$

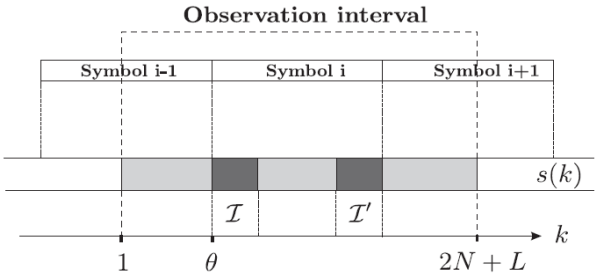

Figure 3: Structure of OFDM signal with cyclicly extended symbols, *s*(*k*). The set *I* contains the cyclic prefix, *i.e.* the copies of the *L* data samples in *I'*.

(see Figure 3). The set I0 thus contains the indices of the data samples that are copied into the cyclic prefix, and the set *I* contains the indices of this prefix. Collect the observed samples in the (2*N* +*L*)*1 -vector $r \triangleq [r(1) \ldots r(2N+L)]^T$. Notice that the samples in the cyclic prefix and their copies, *r*(*k*); $k \in I \cup I'$, are pair wise correlated, *i.e.*,

$$\forall k \in I: \quad E\{r(k) r^*(k+m)\} = \begin{cases} \sigma_s^2 + \sigma_n^2 & m = 0 \\ \sigma_s^2 e^{-j2\pi\varepsilon} & m = N \\ 0 & otherwise \end{cases} \qquad (4)$$

while the remaining samples *r*(*k*); *k* =2 *I [I0* are mutually uncorrelated.

The log-likelihood function for θ and ε, $\Lambda(\theta, \varepsilon)$, is the logarithm of the probability density

function $f\left(r\middle|\theta,\varepsilon\right)$ of the 2*N* + *L* observed samples in **r** given the arrival time μ and the carrier frequency offset ε. In the following, we will drop all additive and positive multiplicative constants that show up in the expression of the log-likelihood function, since they do not affect the maximizing argument. Moreover, we drop the conditioning on (θ,ε) for notational clarity. Using the correlation properties of the observations **r**, the log-likelihood function can be written as

$$\begin{aligned}\Lambda(\theta,\varepsilon)&=\log f\left(r/\theta,\varepsilon\right)\\&=\log\left(\prod_{k\in I}f\left(r(k),r(k+N)\right)\prod_{k\notin I\cup I'}f\left(r(k)\right)\right)\\&=\log\left(\prod_{k\in I}\frac{f\left(r(k),r(k+N)\right)}{f\left(r(k)\right)f\left(r(k+N)\right)}\prod_{k}f\left(r(k)\right)\right),\end{aligned}\qquad(5)$$

where $f(\cdot)$ denotes the probability density function of the variables in its argument. Notice that it is used for both one- and two-dimensional (1-D and 2-D) distributions. The product $\Pi_k f\left(r(k)\right)$ in (4) is independent of θ (since the product is over all *k*) and ε (since the density *f*(*r*(*k*)) is rotationally invariant). Since the ML estimation of θ and ε is the argument maximizing $\Lambda(\theta,\varepsilon)$, we may omit this factor. Under the assumption that **r** is a jointly Gaussian vector, (4) is shown in the Appendix to be

$$\Lambda(\theta,\varepsilon)=\left|r(\theta)\right|\cos\left(2\pi\varepsilon+\angle\gamma(\theta)\right)-\rho\Phi(\theta)\qquad(6)$$

where 6 denotes the argument of a complex number,

$$\gamma(m)\triangleq\sum_{k=m}^{m+L-1}r(k)r^{*}(k+N),\qquad(7)$$

$$\Phi(m)\triangleq\frac{1}{2}\sum_{k=m}^{m+L-1}\left|r(k)\right|^{2}+\left|r(k+N)\right|^{2}\qquad(8)$$

and

$$\rho\triangleq\left|\frac{E\left\{r(k)r^{*}(k+N)\right\}}{\sqrt{E\left\{\left|r(k)\right|^{2}\right\}E\left\{\left|r(k+N)\right|^{2}\right\}}}\right|=\frac{\sigma_s^2}{\sigma_s^2+\sigma_n^2}=\frac{SNR}{SNR+1}\qquad(9)$$

is the magnitude of the correlation coefficient between *r*(*k*) and *r*(*k*+*N*). The first term in (5) is the weighted magnitude of $\gamma(\theta)$, a sum of *L* consecutive correlations between pairs of samples spaced *N* samples apart. The weighting factor depends on the frequency offset. The term $\Phi(\theta)$ is an energy term, independent of the frequency offset ε. Notice that its contribution depends on the SNR (by the weighting-factor ρ).

The maximization of the log-likelihood function can be performed in two steps:

$$\max_{(\theta,\varepsilon)}\Lambda(\theta,\varepsilon)=\max_{\theta}\max_{\varepsilon}\Lambda(\theta,\varepsilon)=\max_{\theta}\Lambda\left(\theta,\hat{\varepsilon}_{ML}(\theta)\right).\qquad(10)$$

The maximum with respect to the frequency offset ε is obtained when the cosine term in (5) equals one. This yields the ML estimation of ε

$$\hat{\varepsilon}_{ML}(\theta)=-\frac{1}{2\pi}\angle\gamma(\theta)+n,\qquad(11)$$

where *n* is an integer. A similar frequency offset estimator has been derived in [11] under different assumptions. Notice that by the periodicity of the cosine function, several maxima are found. We assume that an acquisition, or rough estimate, of the frequency offset has been performed and that $|\varepsilon|<1/2$; thus *n* = 0. Since $\cos\left(2\pi\hat{\varepsilon}_{ML}(\theta)+\angle\gamma(\theta)\right)=1$, the log-likelihood function of θ (which is the compressed log-likelihood function with respect to ε) becomes

$$\Lambda\left(\theta,\hat{\varepsilon}_{ML}(\theta)\right)=\left|\gamma(\theta)\right|-\rho\Phi(\theta)\qquad(12)$$

and the joint ML estimation of θ and ε becomes

$$\hat{\theta}_{ML}=\arg\max_{\theta}\left\{\left|\gamma(\theta)\right|-\rho\Phi(\theta)\right\},\qquad(13)$$

$$\hat{\varepsilon}_{ML}=-\frac{1}{2\pi}\angle\gamma\left(\hat{\theta}_{ML}\right).\qquad(14)$$

ML Estimation of Time and Frequency Offset in OFDM Systems

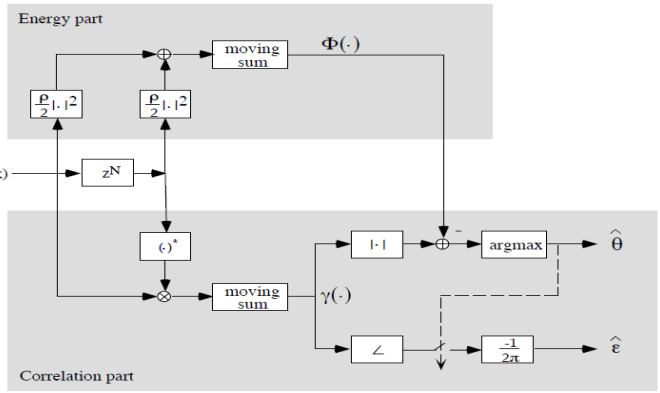

Figure 4: Structure of the estimator.

Notice that only two quantities affect the log-likelihood function (and thus the performance of the estimator): the number of samples in the cyclic prefix *L* and the correlation coefficient ½ given by the SNR. The former is known at the receiver, and the latter can be fixed. Basically, the quantity $\gamma(\theta)$ provides the estimates of μ and ε . Its magnitude, compensated by an energy term, peaks at time instant $\hat{\theta}_{ML}$, while its phase at this time

instant is proportional to $\hat{\varepsilon}_{ML}$. If ε is *a priority* known to be zero, the log-likelihood function for θ becomes $\Lambda(\theta) = \mathrm{Re}\{\gamma(\theta)\} - \rho\Phi(\theta)$ and $\hat{\theta}_{ML}$ is its maximizing argument. This estimator and a low-complexity variant are analyzed in [9]. In an OFDM receiver, the quantity $\gamma(\theta)$, which is defined in (6), is calculated on-line, *cf.* Figure 3. The signals $\Lambda\left(\theta, \hat{\varepsilon}_{ML}(\theta)\right)$ (whose maximizing arguments are the time estimates $\hat{\theta}_{ML}$) and $-\left(1/2\pi\right)\angle\gamma(\theta)$ (whose values at the time instants $\hat{\theta}_{ML}$ yield the frequency estimates) are shown in Figure 4. Notice that (12) and (13) describe an open-loop structure. Closed-loop implementations based on (5) and (11) may also be considered. In such structures the signal $\Lambda\left(\theta, \hat{\varepsilon}_{ML}(\theta)\right)$ is typically fed back in a *phase-locked loop* (PLL). If we can assume that μ is constant over a certain period, the integration in the PLL can significantly improve the performance of the estimators.

III. Results and Conclusion

The objective of our project was to investigate the effects of frequency offset using frequency offset estimation techniques in generalized fading channels of a cellular environment. The objective was accomplished by investigating the effects of frequency offset on OFDM systems, ML estimator for time and frequency offset and preamble usage in frequency offset estimation.

A. Summary Of Work Performed

We presented three methods for frequency offset estimation: data-driven, blind and semi-blind. The data-driven and semi-blind rely on the repetition of data, while the blind technique determines the frequency offset from the QPSK data.

The MATLAB codes presented in Appendix A, B gives the SNR degradation caused by the frequency offset and the offset estimation using the preamble at the beginning of the data.ML estimation of time and frequency offset are given in Appendix C.

B. Significant Results and Conclusions

Simulation results demonstrated the distortive effects of frequency offset on OFDM signals; frequency offset affects symbol groups equally. Additionally, it was seen that an increase in frequency offset resulted in a corresponding increase in these distortive effects and caused degradation in the SNR of individual OFDM symbols.

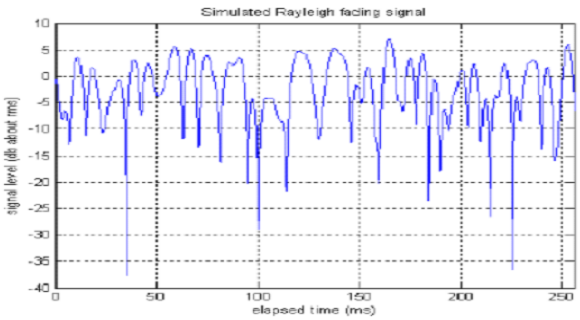

Fig: 5 A typical Rayleigh Fading Envelope

The Rayleigh distribution is commonly used to describe the statistical time varying nature of the received signal power. It describes the probability of the signal level being received due to fading.

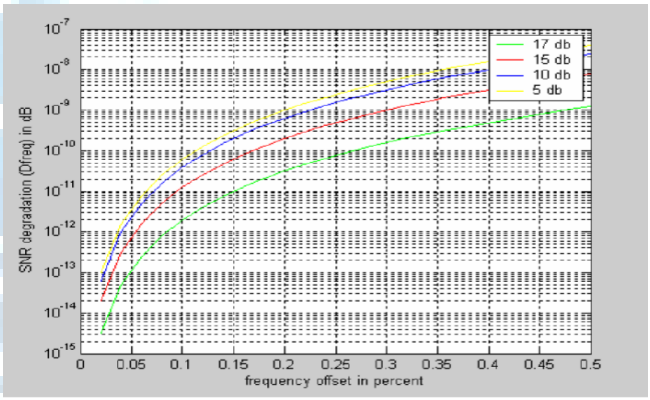

Figure:6 SNR degradation of frequency offset for different $\frac{E_b}{N_o}$ values

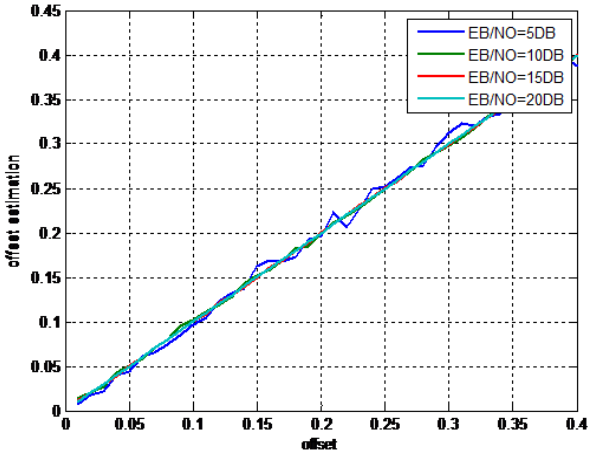

Figure 7: the graph between offset and offset estimation

Figure shows the graph between offset and offset estimation. Higher the SNR value then the graph will be more linear. when the SNR value decreases the graph will be distorted.

Figure below shows the calculated degradation of the SNR due to the frequency offset. For smaller SNR values, the degradation is less than for bigger SNR values as shown in Figure below.

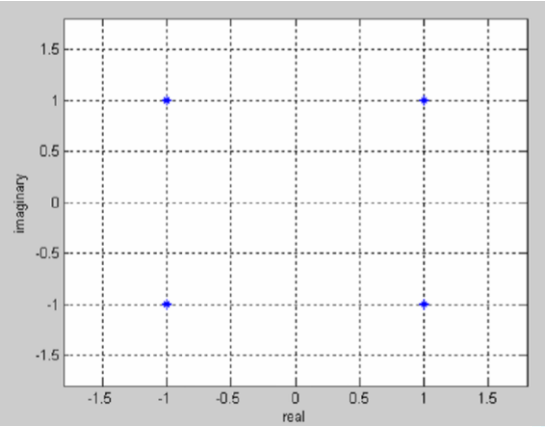

Figure:8 Received signal constellation with 0% frequency offset

Figure below shows under these ideal conditions the received signal constellation in the absence of frequency offset. Since there is no frequency offset or noise it is seen that there is no ICI and no interference between the data and the other zeros.

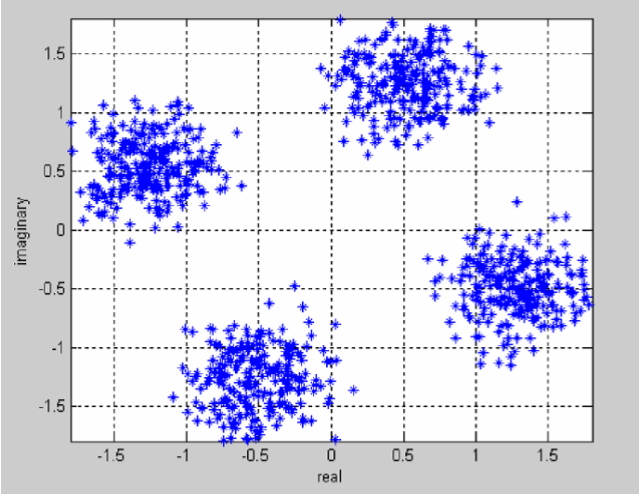

Figure:9 Received signal constellation with 0.3% frequency offset

When frequency offset is introduced in the carrier, its effects are observed in terms of ICI. The result with 0.3% frequency offset is shown in Figure below. In particular we can see that the signal from neighboring carriers causes interference and we have a distorted signal constellation at the receiver.

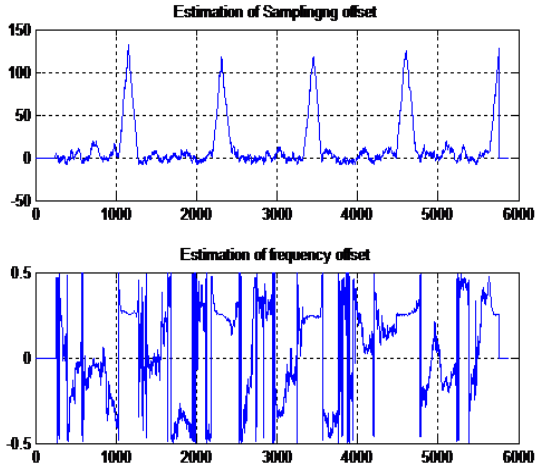

Figure 10: The signals that generate the ML-estimates of (top) and (bottom) yield

In the above figure we are observing the plots of carrier frequency offset and sampling frequency offset. The graph indicates joint clock estimation of CFO and SFO. Here the pulses are varying at the peak position

IV. Conclusion

The data-driven method performed best in terms of frequency offset estimate. However, it requires the data to be repeated twice, which affects the data rate. The blind method is sensitive to noise, but it performs satisfactorily with high SNR.

The use of preambles in frequency offset estimation was also examined. It was seen that the use of preambles and cyclic prefixes increase the robustness of the frequency offset estimation on that user data which comes after the preamble.

.

References

[1] IEEE P802.16e/D4, Draft IEEE Standard for Local and Metropolitan Area Networks-Part 16: Air Interface for Fixed and Mobile Broadband Wireless Access Systems Aug. 2004.

[2] P. H. Moose, "A technique for orthogonal frequency division multiplexing frequency offset correction," IEEE Trans. Commun., vol. 42, no. 10, pp. 2908–2914, Oct. 1994.

[3] M. Sandell, J. Van de Beek, and P. O. Borjesson, "Timing and frequency synchronization in OFDM systems using the cyclic prefix," in Proc. ICUPC '95, Nov. 1995.

[4] T. M. Schmidl and D. C. Cox, "Robust frequency and timing synchronization for OFDM," IEEE Trans. Commun., vol. 45, no. 12, Dec. 1997.

[5] B. Yang, K. B. Letaidf, R. S. Cheng, and Z. Cao, "Timing recovery for OFDM transmission," IEEE J. Sel. Areas Commun., vol. 18, no. 11, Nov. 2000.

[6] D. Matic, N. Petrochilos, and A. Trindade, "OFDM synchronization based on the phase rotation of sub-

carriers," IEEE VTC'00, pp. 1260–1264, Spring, 2000.
[7] M. Sliskovic, "Sampling frequency offset estimation and correction in OFDM systems," in Proc. 8th IEEE ICECS, Malta, 2001.
[8] W. Xiang and T. Pratt, "A simple cascade carrier frequency and sampling clock offsets estimation method for OFDM system," in Proc. IEEE Consumer Commun. Networking Conf., Jan 2004, pp. 718–720.
[9] S. Y. Liu and J. W. Chong, "A study of joint tracking algorithms of carrier frequency offset and sampling clock offset for OFDM-based WLANs," IEEE ICC, CSWSE, vol. 1, pp. 109–113, 2002.
[10] [R. Heaton and B. Hodson, "A fine frequency and fine sample clock estimation technique for OFDM systems," in IEEE VTC'01, Rhodes, Greece, May 2001.
[11] W. Lei, W. Cheng, and L. Sun, "Improved joint carrier and sampling frequency offset estimation scheme for OFDM systems," IEEE GLOBECOM'03, vol. 4, pp. 2315–2319, Dec. 2003.
[12] G. L. Stüber, S. W. McLaughlin, and M. A. Ingram, "Broadband MIMO-OFDM wireless communications," Proc. IEEE, vol. 92, pp. 271–294, Feb. 2004.